ANTIOXIDANTS & REDOX SIGNALING
Volume 11, Number 10, 2009

DOI: 10.1089/ars.2009.2681

Hepatic Ischemia Induced Immediate Oxidative Stress after Reperfusion and Determined the Severity of the Reperfusion-Induced Damage

Sanae Haga,[1,2] S. James Remington,[3] Naoki Morita,[4] Keita Terui,[5] and Michitaka Ozaki[1]

Abstract

Noninvasive evaluation of organ redox states provides invaluable information in many clinical settings. We evaluated a newly developed reduction/oxidation–sensitive green fluorescent protein (roGFP) probe that reports cellular redox potentials and their dynamic changes in live cells. On hypoxia/reoxygenation (H/R) of AML12 liver cells, roGFP indicated mild reduction during hypoxia, but immediate transient oxidation after reoxygenation. The roGFP probe confirmed the antioxidative effects of *N*-acetylcysteine, catalase, redox factor-1, and Mn-SOD/CuZn-SOD against H/R-induced cellular oxidative stress (OS). In a mouse liver ischemia/reperfusion (I/R) model, roGFP transduced by using an adenoviral vector revealed immediate reduction of the liver under ischemia, and two distinct peaks of OS: (a) early, observed within 60 min after reperfusion, similar to the *in vitro* study; and (b) later, at 24 h. The early peak levels paralleled the ischemic time up to 75 min and the postischemic liver injury (sGOT/GPT/LDH) in the later phase (6 and 24 h after I/R). The roGFP probe successfully indicated postischemic OS of the liver in living mice, accurately predicting postischemic liver injury. This probe may represent an effective OS marker indicating organ redox states and also predicting the damage/function. *Antioxid. Redox Signal.* 11, 2563–2572.

Introduction

Ischemia/reperfusion (I/R) is an unavoidable event in liver surgery and transplantation but sometimes causes serious damage by oxidative stress. *In vivo* evaluation of redox states and oxidative stress (OS)-induced liver damage and prediction of postoperative liver function/damage is of grave clinical concern.

Reactive oxygen species (ROS) generated during I/R of the organs certainly account for the majority of I/R-induced cell and organ injury (1, 21, 26). Hepatic I/R results in massive cell death by (a) ROS-mediated immediate apoptosis in the early phase (24), and (b) neutrophil-mediated necrotic cell death in the later phase (15, 17). According to numerous studies of hypoxia/reoxygenation (H/R), a simple *in vitro* model of the early I/R damage, cell injury at the early post-H/R period is definitely mediated by the cellular generation of ROS (8, 22). One of the major sources of cellular ROS generated immediately after H/R may be functionally impaired mitochondria (5, 25). ROS generation associated with Rac1 has also been reported to mediate cellular OS after H/R and I/R (19, 20), which consequently activates redox-dependent pathologic signals, including NF-κB (20).

It is also well known that excessive ROS exert direct deleterious effects on cells through lipid peroxidation, protein degradation, and DNA damage (3, 4). Redox-sensitive signaling molecules such as NF-κB, AP-1, and some mitogen-activated protein kinases (MAPKs) are believed to be activated under these conditions and to play pivotal roles in I/R-induced injury (23). Therefore, regulating the cellular redox state by suppressing cellular ROS in the postischemic tissue has been one of the most promising therapeutic strategies for protection against I/R-induced injury (7). These considerations suggest that the postischemic redox state may be an indicator of liver viability, as well as functional status and degree of damage after liver surgery, implying that their *in vivo* monitoring may provide more diagnostic and therapeutic options in clinical liver surgery and transplantation.

[1]Department of Molecular Surgery, Hokkaido University School of Medicine, Sapporo; and [2]The Japan Society for the Promotion of Science (JSPS), Tokyo, Japan.
[3]Institute of Molecular Biology, Howard Hughes Medical Institute and Department of Physics, University of Oregon, Eugene, Oregon.
[4]Research Institute of Genome-based Biofactory, National Institute of Advanced Industrial Science and Technology (AIST), Sapporo; and [5]Department of Pediatric Surgery, Chiba University Graduate School of Medicine, Chiba, Japan.

For *in vivo* assays of OS, tissues are usually homogenized and subsequently assayed, either with redox-sensing electrodes, or by measuring the ratios of the reduced and oxidized forms of glutathione and ascorbate, two principal redox regulators in living systems (6). Recently, the redox state of tissues has also become assessible by using the dyes 5- (and 6-) carboxy-2,7-dichlorodihydrofluorescein diacetate (11) and dihydrofluorescein diacetate (13). Although such approaches allow us to evaluate the sum of oxidized and reduced species present, and thereby to estimate the overall redox status of the tissue, these techniques do not allow measurement of redox potentials in real time. More important, homogenizing a tissue precludes the possibility of monitoring dynamic changes of redox status, including reversibility.

In the present study, we evaluated a newly developed redox-sensitive green fluorescent protein probe (roGFP probe, GFP with mutations C48S, S147C, Q204C, and S65T) (2, 9) in *in vitro* H/R experiments and in an *in vivo* mouse hepatic I/R model. Use of the roGFP probe enabled us to evaluate cellular/organ redox states noninvasively and continuously. Adenovirally transduced roGFP in the liver was shown to act as an indicator of pre- and postischemic redox states, and to predict subsequent I/R-induced liver damage. Thus, by using this roGFP probe, postoperative liver damage/function could be predicted by the noninvasively detected postischemic redox state.

Materials and Methods

Redox-sensitive roGFP probe

Redox-sensitive GFPs, which allow real-time visualization of the oxidation/reduction potentials of various cells *in vitro*, have been developed and reported recently (2, 9). The indicator examined in this work is a GFP mutant with two surface-exposed cysteines at positions 147 and 204 on adjacent β-strands close to the chromophore (Fig. 1). Disulfide-bond formation between the cysteine residues promotes protonation of the chromophore, increases the excitation spectrum peak near 400 nm, and reduces the excitation spectrum peak near 480 nm. Thus, by calculating the ratios of fluorescence intensities from excitation at 400–480 nm [(em. 530 nm at ex. 400 nm)/(em. 530 at ex. 480 nm)], an indication of the redox potential can be derived and hence the extent of oxidation. Hereafter, redox status is expressed as a ratio of emitted signals at 535 nm from ex. 400 nm and ex. 480 nm (ratio ex 400/480 nm), unless otherwise noted.

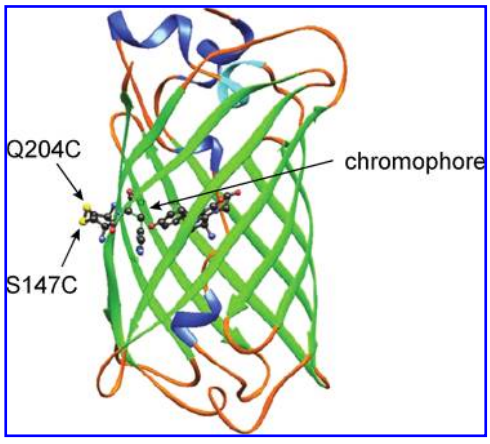

FIG. 1. A structural feature of roGFP. The engineered cysteines Q204C/S147C form a disulfide crosslink between adjacent β-strands near the chromophore in GFP. The figure is modified from the original (9). (For interpretation of the references to color in this figure legend, the reader is referred to the web version of this article at www.liebertonline.com/ars).

In vitro *imaging of AML12 liver cells challenged with oxidizing/reducing agents and H/R*

AML12 (alpha mouse liver 12) cells (ATCC, Manassas, VA), established from hepatocytes from a mouse transgenic for human transforming growth factor-α (TGF-α), express high levels of human TGF-α and lower levels of mouse TGF-α. AML12 cells were maintained at 37°C in 5% CO_2 in DMEM/F12 (Invitrogen, Carlsbad, CA) supplemented with 10% fetal bovine serum. A replication-deficient recombinant adenovirus encoding *roGFP* (Ad*roGFP*) was generated and transfected into AML12 cells at 5 moi (multiplicities of infection) 48 h before use.

AML12 cells were subjected to an oxidizing agent [4,4-dithiodipyridine (Aldrithiol, AT-4), a reducing agent (dithiothreitol; DTT), or H/R. To simulate *in vivo* liver ischemia, cellular hypoxic conditions were created and maintained in a stage-top incubator (Tokai Hit, Shizuoka, Japan) set in the fluorescence microscope BZ-8000 (KEYENCE, Osaka, Japan) by continuous gas flow with a 95% N_2/5% CO_2 gas mixture (150 ml/min). This method has been shown to achieve a po_2 of 10 ± 5 Torr (where 1 Torr = 0.133 kPa) within 2 min (19). After hypoxia of AML12 cells, reoxygenation was achieved by continuously flushing with a 95% air/5% CO_2 gas mixture.

The cellular redox potentials were imaged with fluorescence microscopy during challenge with the oxidizing/reducing agents and H/R with an emission wavelength of 530 nm and excitation wavelengths of 400/480 nm, as mentioned earlier. Fluorescence intensities resulting from excitation at 480/400 nm were quantified by using BZ-analyzer software (KEYENCE). In each experiment, at least 20 cells were measured, and the ratio ex 400/480 nm was used as a cellular redox index.

In vivo *imaging of mouse liver challenged with I/R*

Male C57Black/6 mice, 8–10 weeks old, were starved overnight before use. Three days before each experiment, Ad*roGFP* was administered intravenously (IV) *via* the tail vein in a volume of 100 μl (1×10^8 pfu/body) by using a 31G needle. Ad*roGFP* was also subcutaneously injected (0.5×10^8 pfu/30 μl) in the chest after shaving hair, to normalize the signals from the liver, because the expression levels of adenovirally induced roGFP will change with time. Adenovirus encoding β-galactosidase was used as a control vector. Adenoviral vectors encoding cDNAs of redox factor-1 (Ad*Ref-1*) and superoxide dismutases (Ad*Mn-SOD* and Ad*Cu/Zn-SOD*) were previously described (27).

General anesthesia was induced with the inhalation anesthetic methoxyflurane (Metofane), and heparin sulfate (100 U/kg body weight) was intravenously injected. After laparotomy, all vessels (hepatic artery, portal vein, and bile duct) to the left and median liver lobes were clamped, according to a previously described method (20). After 30–90 min of liver partial ischemia, these vessels were unclamped, and the hepatic circulation was restored for the specified reperfusion period.

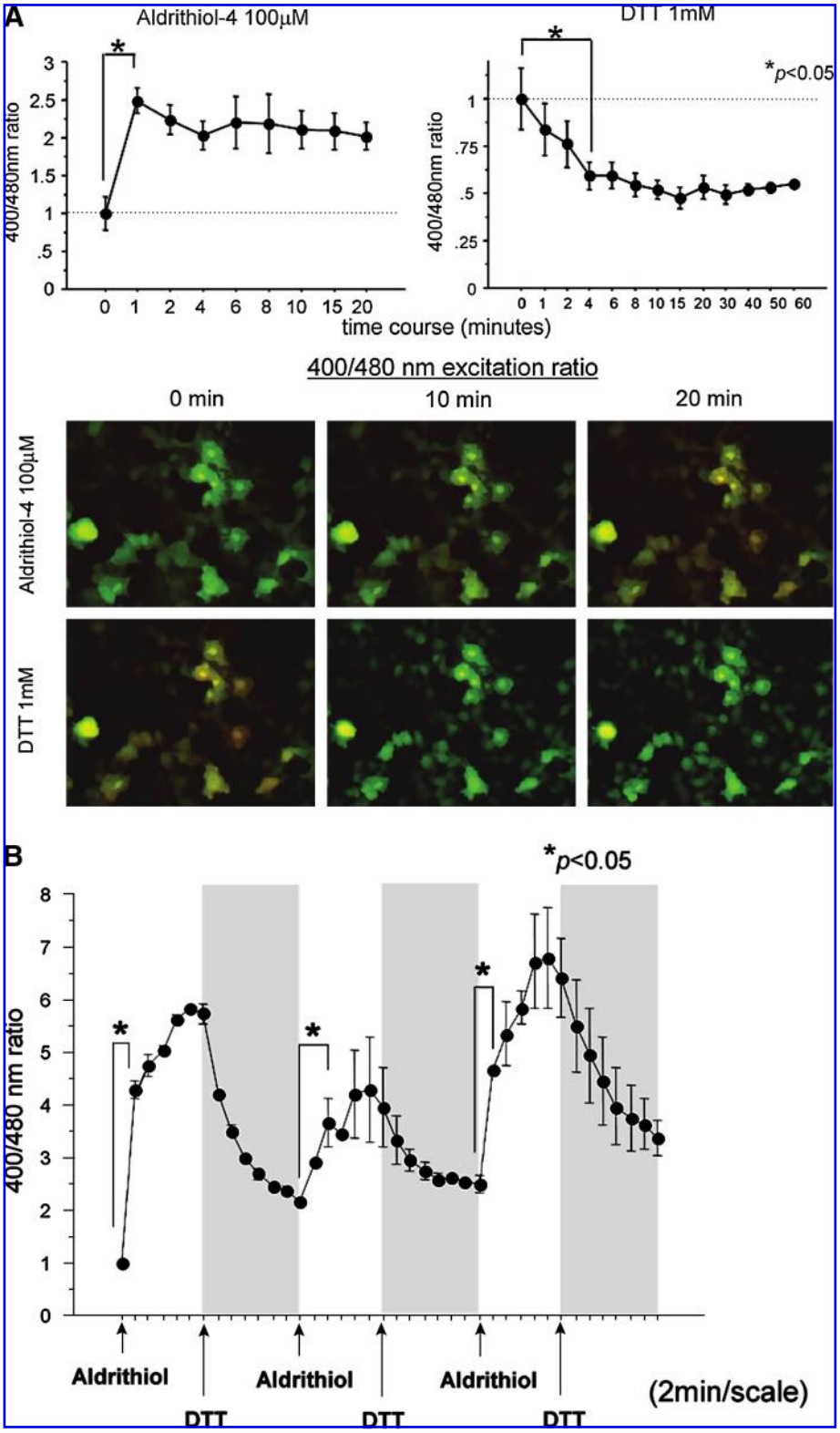

FIG. 2. roGFP reports dynamic changes of redox states caused by Aldrithiol-4 and dithiothreitol (DTT) treatment in live hepatocytes. The cellular redox states were imaged with fluorescence microscopy during challenge with the oxidizing and reducing agents Aldrithiol-4 and DTT, respectively. (**A**) The ratios of fluorescence intensities emitted at 535 nm from excitations at 480/400 nm were calculated and expressed as 400/480 nm ratios (cellular redox indices). Hepatocytes transfected with the roGFP probe showed oxidation and reduction in response to Aldrithiol-4 and DTT. Oxidation, yellow; reduction, green, pseudocolor. (**B**) roGFP continuously manifested changes of oxidation and reduction in response to alternating repetitive treatment with Aldrithiol-4 and DTT. Data were from at least three independent experiments, expressed as mean ± SEM. (For interpretation of the references to color in this figure legend, the reader is referred to the web version of this article at www.liebertonline.com/ars).

For *in vivo* liver imaging, the organ was exposed under anesthesia to enable a CCD camera to record liver images directly. *In vivo* imaging of the mouse liver was performed by using a *Photon Imager* (Biospace Lab, Paris, France). In the *in vivo* study, fluorescence intensities at 530 nm from excitation at 480 nm were measured and reciprocally plotted [1/(em. 530 at ex. 480 nm)]. This allows the signal to increase with oxidation and to decrease with reduction and can be used as an index of an *in vivo* redox state. The *in vivo* roGFP signals from the liver were normalized against the control roGFP signals from the chest.

All animals were handled according to uniform policies set forth by the Animal Care and Use Committee of The Hokkaido University School of Medicine.

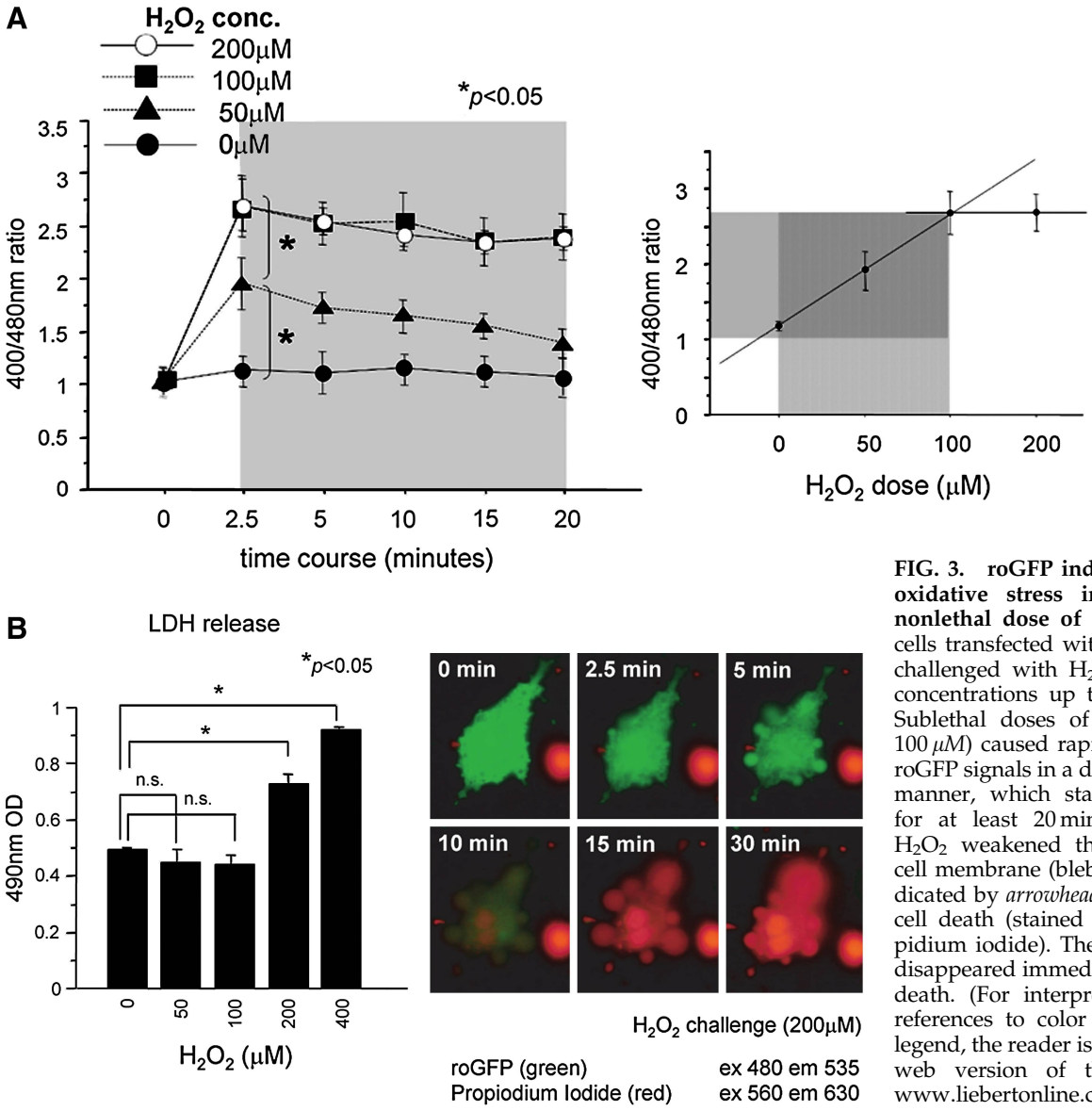

FIG. 3. roGFP indicates cellular oxidative stress induced by a nonlethal dose of H_2O_2. AML12 cells transfected with roGFP were challenged with H_2O_2 at various concentrations up to 200 μM. (**A**) Sublethal doses of H_2O_2 (up to 100 μM) caused rapid elevation of roGFP signals in a dose-dependent manner, which stably continued for at least 20 min. (**B**) 200 μM H_2O_2 weakened the integrity of cell membrane (bleb formation indicated by *arrowheads*) and caused cell death (stained red with propidium iodide). The roGFP signal disappeared immediately after cell death. (For interpretation of the references to color in this figure legend, the reader is referred to the web version of this article at www.liebertonline.com/ars).

Biochemical measurement of oxidative stress and apoptosis in liver tissue

For evaluation of apoptotic cell death of the liver tissue, an ELISA kit (Cell Death Detection ELISA^{PLUS}; Roche, Basel, Switzerland) was used according to the manufacturer's instructions. Biochemical analyses, such as tissue 4-hydroxy-2-nonenal (4-HNE) as a peroxidation index and serum GOT/GPT/LDH levels as liver-damage indices, were performed at the time points indicated before and after reperfusion. For Western blot analysis, anti-4-HNE was purchased from Japan Institute for the Control of Aging (JaICA, Shizuoka, Japan).

Statistical analysis

Results are expressed as means ± SEM. Statistical analyses were performed with the Fisher test, and p values less than 0.05 were considered significant.

Results

roGFP is an indicator of cellular oxidation and reduction by Aldrithiol-4 and DTT, respectively, in hepatocytes

To validate the roGFP probe as a redox indicator, we first performed an *in vitro* study with AML12 liver cells. AML12 cells transfected with roGFP were challenged with an oxidizing agent, 4,4-dithiodipyridine, AT-4; Aldrithiol-4) and a reducing agent, DTT (Fig. 2A). Signals emitted from AML12 cells were instantly increased by a single addition of Aldrithiol-4 and gradually decreased again over the next 20 min. In contrast, the addition of DTT to these AML12 cells resulted in a slow and steady reduction of the roGFP signal. Moreover, roGFP was also able to indicate changes of oxidation and reduction in response to repeated alternating administration of Aldrithiol-4 and DTT (Fig. 2B). Thus, the roGFP probe could detect repeated OS events and allowed good visualization of chemically induced cellular redox changes.

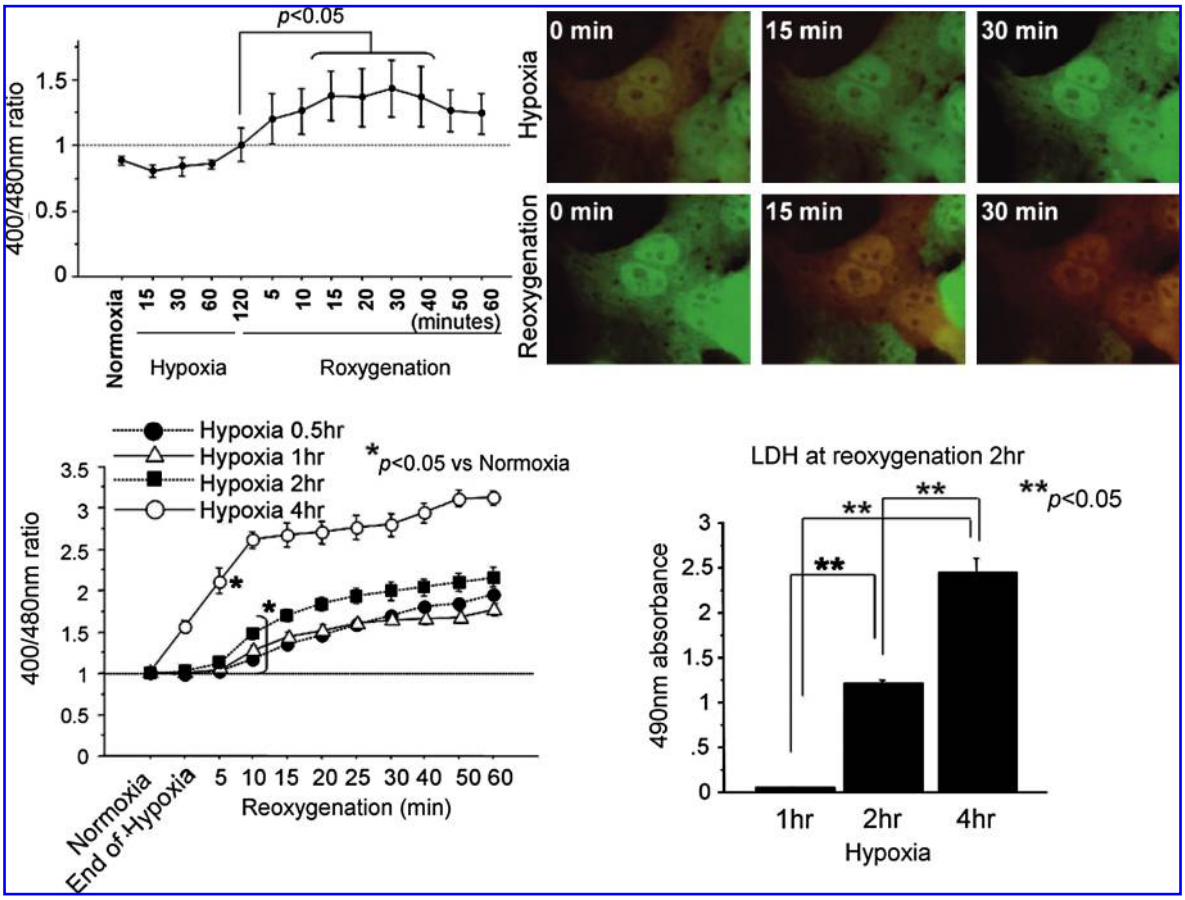

FIG. 4. roGFP reports dynamic changes of hypoxia/reoxygenation (H/R)-induced oxidative stress. AML12 cells transfected with roGFP were challenged by H/R. During hypoxia, roGFP reports mild reduction (green) and rapid oxidation (yellow) immediately after reoxygenation (*upper panel*). Posthypoxic early oxidative stress paralleled subsequent cell injury (*lower panel*). Data were from at least three independent experiments, expressed as mean ± SEM. (For interpretation of the references to color in this figure legend, the reader is referred to the web version of this article at www.liebertonline.com/ars).

Redox changes of hepatocytes by hypoxia/reoxygenation and cell death

We next examined whether the roGFP probe can act as an indicator of physiopathologic OS in AML12 cells. First, AML12 cells were directly challenged with different concentrations of H_2O_2 up to 200 μM (Fig. 3A). The roGFP probe reported cellular OS under subtoxic doses of H_2O_2 (in a dose-dependent manner up to 100 μM) with a signal intensity stable for at least 20 min. Concentrations of H_2O_2 greater than 200 μM induced cell death (Fig. 3B left panel), accompanied by reduced integrity of the cell membrane (blebbing) and death within 20 min (as shown by propidium iodide incorporation, Fig. 3B right panel). At this high concentration, cells may not be able to emit roGFP signals because the probe is dispersed in the culture medium after membrane disintegration.

Next, AML12 cells transfected with roGFP were subjected to 2 h of hypoxia followed by reoxygenation (Fig. 4, upper panel). AML12 cells showed a mildly reduced status during hypoxia, but then somewhat oxidized at the end of hypoxia. Cells were oxidized promptly after reoxygenation. The posthypoxic OS peaked within 60 min, and thereafter gradually reduced to basal levels. In addition, the OS peak values observed early after hypoxia paralleled the hypoxic time (up to 4 h) and were also indicative of subsequent cell damage (Fig. 4, lower panel).

These data show that roGFP acts as an indicator of cellular OS in various physiopathologic conditions in live cells, which reflects OS-induced cellular damage.

Evaluation of the effects of antioxidants on H/R-induced OS

We next evaluated the efficacy of various antioxidant drugs/proteins on H/R-induced OS in AML12 cells by using this redox-sensitive probe (Fig. 5). *N*-Acetylcysteine (NAC) and catalase, added before hypoxia, equally and very effectively suppressed H/R-induced OS (Fig. 5, upper panel). To examine the effects of redox factor-1 (Ref-1), an antioxidant protein, as well as Mn-SOD or Cu/Zn-SOD, adenoviruses coding for *Ref-1* (Ad*Ref-1*), Mn-SOD (Ad*MnSOD*), or Cu/Zn-SOD (Ad*Cu/ZnSOD*) were transfected at 10 moi, resulting in overexpression of the respective gene products in AML12 cells (Fig. 5, lower panel). Ref-1 suppressed H/R-induced OS effectively. Although Cu/Zn-SOD partially suppressed posthypoxic OS, Mn-SOD did not result in any decrease in roGFP signals. This may possibly be explained by roGFP reacting not only with superoxide anion but also with H_2O_2, which is generated from the former by SOD. However, the precise

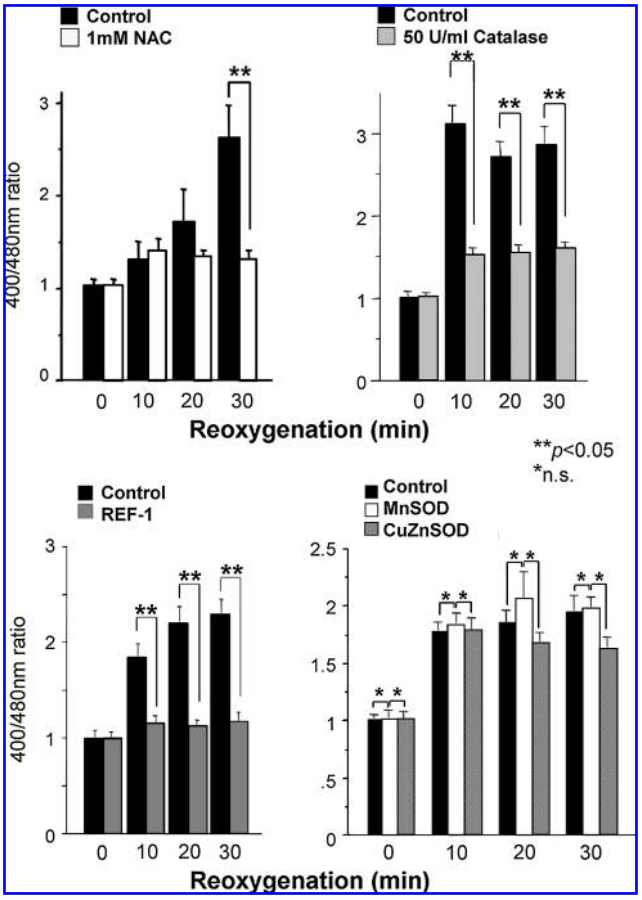

FIG. 5. roGFP indicates the antioxidative effects of NAC/catalase and Ref-1/Mn-SOD/CuZn-SOD on H/R-induced oxidative stress in hepatocytes. AML12 cells transfected with roGFP were challenged with 2 h of hypoxia followed by reoxygenation. *N*-Acetylcysteine (NAC) and catalase were administered 1 h before hypoxia (*upper panel*). Both NAC and catalase suppressed posthypoxic early OS effectively. Adenoviral vectors at 10 moi encoding *Ref-1, Mn-SOD,* or *Cu/Zn-SOD* were used to infect cultures 72 h before hypoxia (*lower panel*). Despite SOD, Ref-1 markedly suppressed posthypoxic OS. Data were from at least three independent experiments, expressed as mean ± SEM.

mechanism whereby Cu/Zn-SOD reduced post-H/R OS more effectively is currently undetermined.

The roGFP probe thus successfully illustrated and validated the effects of these antioxidants on H/R-induced OS in the *in vitro* experiments.

In vivo *redox monitoring of the liver during ischemia/reperfusion in mice*

To validate the *in vivo* usefulness of the roGFP probe, we investigated a mouse liver I/R model. Ad*roGFP* (1×10^8 pfu/body) was intravenously injected 72 h before the experiment. Adenovirally transduced roGFP allowed visualization of hepatic redox states during ischemia or reperfusion or both. Figure 6 (upper panel) shows representative images of ischemic and postischemic hepatic redox states in a model of 60-min hepatic ischemia and reperfusion. The liver redox state was promptly shifted to reduction (shown as green to blue) on ischemia, which was stable until the liver was reperfused. After reperfusion, the redox state rapidly shifted to oxidation (shown as orange to red), "an early postischemic OS." This OS persisted for at least 60 min and returned to the preischemic state 4–8 h after I/R. The liver redox state was shifted again to oxidation 24–48 h after I/R, "a late postischemic OS" (Fig. 6). Previous studies reported the same postischemic OS patterns in liver, in agreement with our present data (18).

The early postischemic OS was not marked in livers subjected to 30–45 min of ischemia, but became elevated in parallel with increasing ischemic time, peaking at 75 min (Fig. 6, lower panel). Interestingly, the early postischemic OS reflected liver injury occurring in the later phase (Fig. 7A, upper panel). The second OS in the late phase was strong and of long duration, occurring after only 45 min of ischemia, as well as after 60 and 75 min. After 90 min of hepatic ischemia, however, both the early and late postischemic OS peaks were no longer apparent (Fig. 6). This may be because most liver cells died during 90 min of ischemia.

The postischemic OS reported by roGFP was confirmed by assays of the conventional biochemical oxidative marker, 4-HNE (Fig. 7B). The postischemic OS (4-HNE) and cell-damage markers (caspase-3 activation and GOT/GPT/LDH release) were both elevated in parallel with the ischemic time up to 90 min, as well as the postischemic early OS peaks at least up to 75 min. The early post-I/R peak is NADPH oxidase independent and originates largely from liver parenchymal cells. The later peak is NADPH oxidase-dependent, and originates largely from the hepatic infiltrating neutrophils (neutrophilic oxidative burst) (18). As mentioned earlier, after 90 min of hepatic ischemia, no postischemic OS was detectable, which may be because hepatocytes expressing roGFP were mostly dead after this severe ischemic insult (Fig. 7A, lower panel).

The results with roGFP also validated the antioxidative effect of NAC, a common antioxidant, on the postischemic liver. A single administration of NAC before hepatic ischemia effectively prevented postischemic OS (Fig. 8). NAC also prevented the postischemic liver damage (data not shown).

These data document that the roGFP probe can be used as a good predictive marker of organ damage induced by OS.

Discussion

This is the first study to visualize *in vivo* OS in the postischemic mouse liver. By reporting real-time redox states of the cells/liver, roGFP indicated dynamic changes of OS, which could not have been achieved by the conventional DCFDH/DA reagents (8). Two distinct OS peaks were found after the hepatic I/R, with the first being observed immediately after reperfusion, and the second, 24–48 h thereafter. The early postischemic OS peak essentially paralleled subsequent liver injury (assessed by the increase of 4-HNE, caspase-3 activity, and serum levels of GOT/GPT/LDH). roGFP also reported the effects of various antioxidant agents or proteins on H/R- or I/R-induced damage in hepatocytes and liver, respectively.

In the *in vitro* experiments, the roGFP probe measured cellular OS semiquantitatively in parallel with H_2O_2 concen-

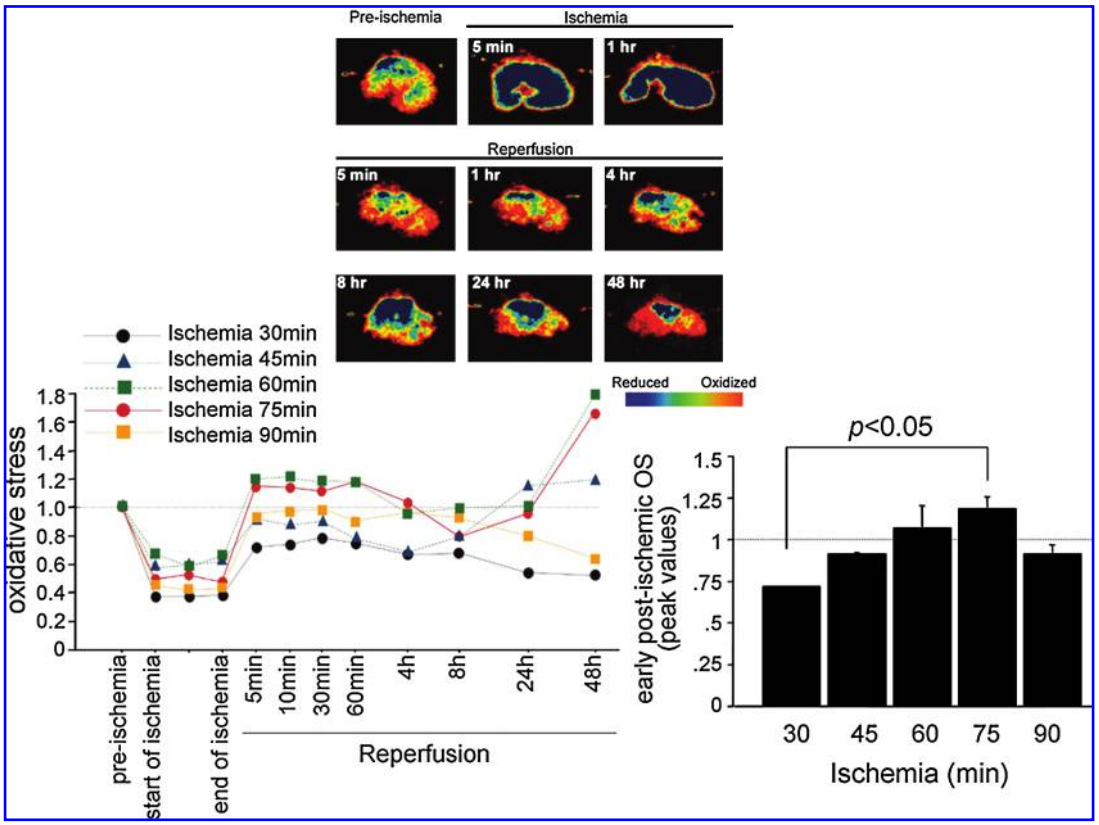

FIG. 6. ***In vivo*** **redox monitoring of the liver during ischemia/reperfusion.** The roGFP probe was intravenously transfected into mouse liver 72 h before the experiment (1×10^8 pfu/body). The liver was then subjected to 2/3 partial ischemia (middle and left lobes) for 30–90 min, followed by reperfusion. The roGFP probe clearly shows dynamic changes of liver redox states. The upper panel depicts representative images of the dynamic changes after 60 min of ischemia followed by reperfusion (reduction, green to blue; oxidation, orange to red). The early postischemic liver OS depended on the ischemic time (*lower panel*). In each experiment, the intensities of the hepatic roGFP signals were plotted relative to the preischemic values. The lines of the graph were plotted as the average values of two independent experiments, and the peak OS values were expressed as mean ± SEM of at least three independent experiments. (For interpretation of the references to color in this figure legend, the reader is referred to the web version of this article at www.liebertonline.com/ars).

trations up to 100 μM. Signals from roGFP, however, reached a plateau at ~100 μM of H_2O_2. At higher concentrations, roGFP no longer indicated OS in proportion to the H_2O_2 concentration. In addition, the roGFP signal disappeared instantly after cell death (Fig. 3B, right panel). This may be because intracellular roGFP disperses into the medium as soon as cell integrity is compromised. Thus, roGFP will be useful to indicate cellular redox status at physiologic and sublethal levels of cellular OS. Likewise, in the *in vivo* experiments, roGFP reported postischemic hepatic OS proportional to the ischemic time up to 75 min, but no longer showed strong OS in the 90 min–reperfused liver, although the conventional biochemical OS marker 4-HNE still did so. This may be because of the extensive cell necrosis due to the prolonged 90-min hepatic ischemia: the roGFP would have been washed away on reperfusion, as suggested in the *in vitro* study.

As mentioned earlier, roGFP validated the action of antioxidant agents/proteins in both hepatocytes and intact liver. NAC, catalase, and Ref-1 were shown to reduce posthypoxic OS effectively in hepatocytes, as expected. However, Mn-SOD and Cu/Zn-SOD failed to suppress the posthypoxic OS effectively, although Cu/Zn-SOD exerted some activity. roGFP may have reacted with H_2O_2 as well as superoxide anion, as SOD will catalyze the generation of H_2O_2 from the latter (16). This idea is supported by the fact that catalase, which further catalyzes H_2O_2 to H_2O, caused a marked decrease in roGFP signals.

Under hypoxic conditions of <2 h duration, roGFP indicated mild cellular reduction in the *in vitro* experiments. However, some reports suggest cellular OS during hypoxia (10, 14). In support of this, roGFP indicated mild cellular oxidation after >2 h of hypoxia. However, roGFP did not reveal OS in the *in vivo* liver ischemia model (up to 90 min), suggesting distinct cellular redox regulatory mechanisms in liver ischemia and cellular hypoxia.

Because of their short wavelengths, the signals emitted by roGFP cannot penetrate far through tissues. Therefore, it may be difficult to apply this probe directly to *in vivo* imaging of deep organs in humans, although this probe can be applied to the organs/tissues other than liver and predict OS-mediated injury. However, for organ transplantation and intraoperative use, this kind of probe will provide many clues for predicting

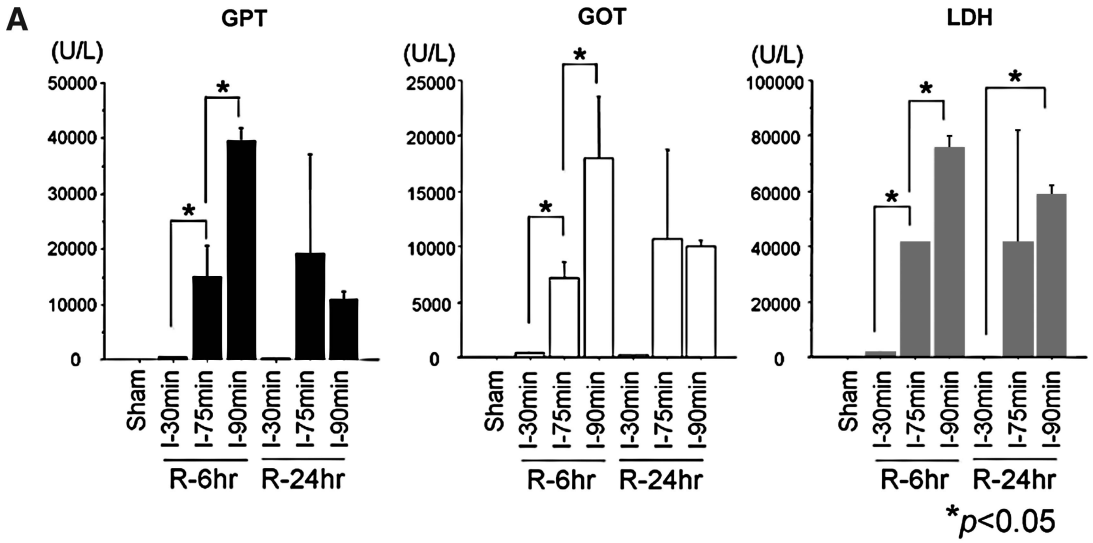

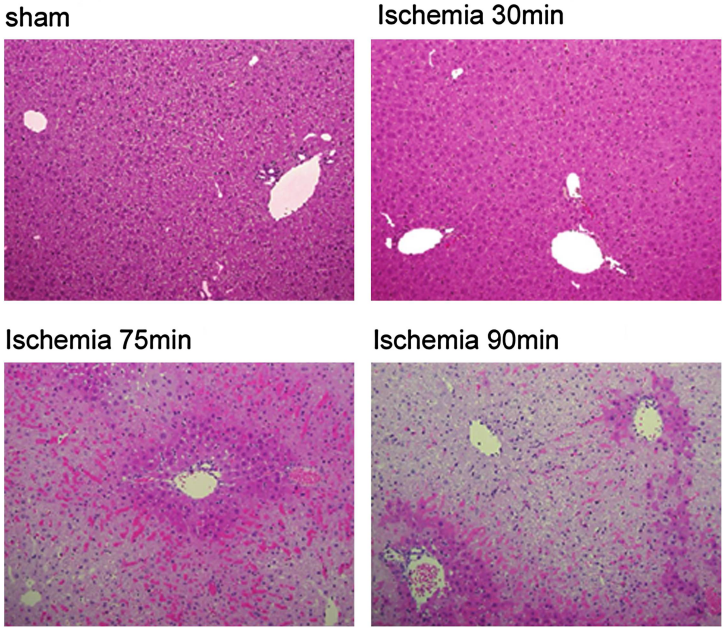

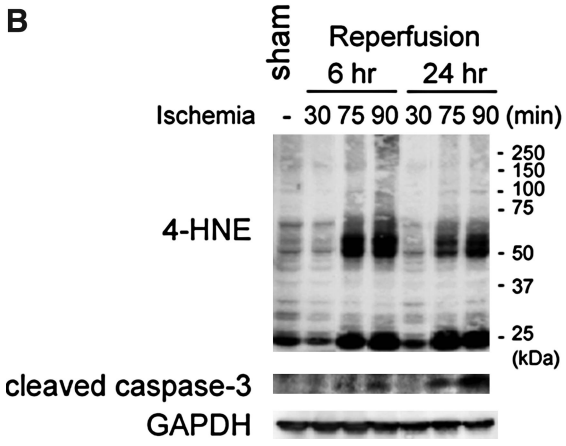

FIG. 7. Postischemic damage and oxidative stress in liver tissue. (**A**) Postischemic liver damage was assessed by the serum levels of GOT/GPT/LDH and histologic analysis (6 h after I/R, H & E; original magnification, ×200). Data were from at least three independent experiments, expressed as mean ± SEM, and each blot is a representative of at least three independent experiments. (**B**) The early postischemic liver OS and subsequent liver injury was evaluated with 4-HNE and caspase-3 activity, respectively. (For interpretation of the references to color in this figure legend, the reader is referred to the web version of this article at www.liebertonline.com/ars).

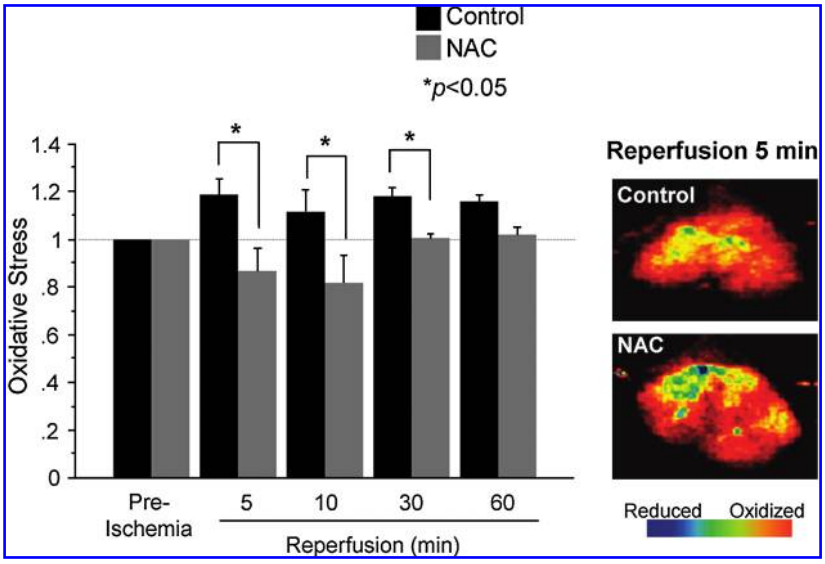

FIG. 8. roGFP quantitatively evaluates the antioxidative efficacy of NAC *in vivo*. NAC (400 mg/kg body weight) was intravenously administrated into mouse 1 h before the experiment. The suppression of postischemic OS by NAC was assessed with an roGFP probe. Data from at least three independent experiments were expressed as mean ± SEM. (For interpretation of the references to color in this figure legend, the reader is referred to the web version of this article at www.liebertonline.com/ars).

organ damage. Especially in liver transplantation, this probe may be very useful to measure postischemic (posttransplant) liver OS noninvasively and to predict posttransplant organ damage (viability).

In conclusion, in the present study, we demonstrated the efficacy of a newly developed roGFP probe capable of reporting redox states in hepatocytes and liver. With this roGFP probe, postoperative liver damage/function could be predicted by a noninvasively detected postischemic redox state.

Acknowledgments

This work was supported by a Grant-in-Aid for Scientific Research from the Ministry of Education, Culture, Sports, Science, and Technology of Japan (17659396, 19659317, and 20249060 to M.O.) and JSPS grant for Young Scientists (S.H.).

Author Disclosure Statement

No competing financial interests exist.

References

1. Andreoli SP. Reactive oxygen molecules, oxidant injury and renal disease. *Pediatr Nephrol* 5: 733–742, 1991.
2. Dooley CT, Dore TM, Hanson GT, Jackson WC, Remington SJ, and Tsien RY. Imaging dynamic redox changes in mammalian cells with green fluorescent protein indicators. *J Biol Chem* 279: 22284–22293, 2004.
3. Droge W. Free radicals in the physiological control of cell function. *Physiol Rev* 82: 47–95, 2002.
4. Droge W and Schipper HM. Oxidative stress and aberrant signaling in aging and cognitive decline. *Aging Cell* 6: 361–370, 2007.
5. Du G, Mouithys-Mickalad A, and Sluse FE. Generation of superoxide anion by mitochondria and impairment of their functions during anoxia and reoxygenation in vitro. *Free Radic Biol Med* 25: 1066–1074, 1998.
6. Dutilleul C, Garmier M, Noctor G, Mathieu C, Chétrit P, Foyer CH, and de Paepe R. Leaf mitochondria modulate whole cell redox homeostasis, set antioxidant capacity, and determine stress resistance through altered signaling and diurnal regulation. *Plant Cell* 15: 1212–1226, 2003.
7. Guo L, Haga S, Enosawa S, Naruse K, Harihara Y, Sugawara Y, Irani K, Makuuchi M, and Ozaki M. Improved hepatic regeneration with reduced injury by redox factor-1 in a rat small-sized liver transplant model. *Am J Transplant* 4: 879–887, 2004.
8. Haga S, Terui K, Fukai M, Oikawa Y, Irani K, Furukawa H, Todo S, and Ozaki M. Preventing hypoxia/reoxygenation damage to hepatocytes by p66(shc) ablation: up-regulation of anti-oxidant and anti-apoptotic proteins. *J Hepatol* 48: 422–432, 2008.
9. Hanson GT, Aggeler R, Oglesbee D, Cannon M, Capaldi RA, Tsien RY, and Remington SJ. Investigating mitochondrial redox potential with redox-sensitive green fluorescent protein indicators. *J Biol Chem* 279: 13044–13053, 2004.
10. Jia L, Xu M, Zhen W, Shen X, Zhu Y, Wang W, and Wang X. Novel anti-oxidative role of calreticulin in protecting A549 human type II alveolar epithelial cells against hypoxic injury. *Am J Physiol Cell Physiol* 294: C47–C55, 2008.
11. Jiang J, Kini V, Belikova N, Serinkan BF, Borisenko GG, Tyurina YY, Tyurin VA, and Kagan VE. Cytochrome c release is required for phosphatidylserine peroxidation during Fas-triggered apoptosis in lung epithelial A549 cells. *Lipids* 39: 1133–1142, 2004.
12. Jiang K, Schwarzer C, Lally E, Zhang S, Ruzin S, Machen T, Remington SJ, and Feldman L. Expression and characterization of a redox-sensing green fluorescent protein (reduction-oxidation-sensitive green fluorescent protein) in *Arabidopsis*. *Plant Physiol* 141: 397–403, 2006.
13. Jones MA, Raymond MJ, Yang Z, and Smirnoff N. NADPH oxidase-dependent reactive oxygen species formation required for root hair growth depends on ROP GTPase. *J Exp Bot* 58: 126–127, 2007.
14. Li C and Jackson RM. Reactive species mechanisms of cellular hypoxia-reoxygenation injury. *Am J Physiol Cell Physiol* 282: C227–C229, 2002.
15. Montalvo-Jave EE, Escalante-Tattersfield T, Ortega-Salgado JA, Pina E, and Geller DA. Factors in the pathophysiology of the liver ischemia-reperfusion injury. *J Surg Res* 147: 153–159, 2008.

16. Morel Y and Barouki R. Repression of gene expression by oxidative stress. *Biochem J* 342: 481–496, 1999.
17. Oreopoulos GD, Wu H, Szaszi K, Fan J, Marshall JC, Khadaroo RG, He R, Kapus A, and Rotstein OD. Hypertonic preconditioning prevents hepatocellular injury following ischemia/reperfusion in mice: a role for interleukin 10. *Hepatology* 40: 211–220, 2004.
18. Ozaki M, Deshpande SS, Angkeow P, Bellan J, Lowenstein CJ, Dinauer MC, Goldschmidt-Clermont PJ, and Irani K. Inhibition of the Rac1 GTPase protects against nonlethal ischemia/reperfusion-induced necrosis and apoptosis in vivo. *FASEB J* 14: 418–429, 2000.
19. Ozaki M, Haga S, Zhang HQ, Irani K, and Suzuki S. Inhibition of hypoxia/reoxygenation-induced oxidative stress in HGF-stimulated antiapoptotic signaling: role of PI3-K and Akt kinase upon rac1. *Cell Death Differ* 10: 508–515, 2003.
20. Ozaki M, Suzuki S, and Irani K. Redox factor-1/APE suppresses oxidative stress by inhibiting the rac1 GTPase. *FASEB J* 16: 889–890, 2002.
21. Robin E, Guzy RD, Loor G, Iwase H, Waypa GB, Marks JD, Hoek TL, and Schumacker PT. Oxidant stress during simulated ischemia primes cardiomyocytes for cell death during reperfusion. *J Biol Chem* 282: 19133–19143, 2007.
22. Terui K, Enosawa S, Haga S, Zhang HO, Kuroda H, Kouchi K, Matsunaga T, Yoshida H, Engelhardt JF, Irani K, Ohnuma N, and Ozaki M. Stat3 confers resistance against hypoxia/reoxygenation-induced oxidative injury in hepatocytes through upregulation of Mn-SOD. *J Hepatol* 41: 957–965, 2004.
23. Thannickal VJ and Fanburg BL. Reactive oxygen species in cell signaling. *Am J Physiol Lung Cell Mol Physiol* 279: L1005–L1028, 2000.
24. Tsung A, Kaizu T, Nakao A, Shao L, Bucher B, Fink MP, Murase N, and Geller DA. Ethyl pyruvate ameliorates liver ischemia-reperfusion injury by decreasing hepatic necrosis and apoptosis. *Transplantation* 79: 196–204, 2005.
25. Weinberg JM, Venkatachalam MA, Roeser NF, and Nissim I. Mitochondrial dysfunction during hypoxia/reoxygenation and its correction by anaerobic metabolism of citric acid cycle intermediates. *Proc Natl Acad Sci U S A* 97: 2826–2831, 2000.
26. Williams EA, Quinlan GJ, Anning PB, Goldstraw P, and Evans TW. Lung injury following pulmonary resection in the isolated, blood-perfused rat lung. *Eur Respir J* 14: 745–750, 1999.
27. Zwacka RM, Zhou W, Zhang Y, Darby CJ, Dudus L, Halldorson J, Oberley L, and Engelhardt JF. Redox gene therapy for ischemia/reperfusion injury of the liver reduces AP1 and NF-kappaB activation. *Nat Med* 4: 698–704, 1998.

Address correspondence to:
Michitaka Ozaki, M.D., Ph.D.
Department of Molecular Surgery
Hokkaido University School of Medicine
N-15, W-7, Kita-ku
Sapporo, Hokkaido, 060-8638 Japan

E-mail: mozaki@m07.itscom.net;
ozaki-m@med.hokudai.ac.jp

Date of first submission to ARS Central, May 28, 2009; date of acceptance, June 2, 2009.

Abbreviations Used

DTT = dithiothreitol
4-HNE = 4-hydroxy-2-nonenal
I/R = ischemia/reperfusion
MAPKs = mitogen-activated protein kinases
NAC = *N*-acetylcysteine
OS = oxidative stress
Ref-1 = redox factor-1
roGFP = reduction/oxidation-sensitive green fluorescent protein
ROS = reactive oxygen species
SOD = superoxide dismutase

This article has been cited by:

1. Frank Funke, Florian J. Gerich, Michael Müller. 2011. Dynamic, semi-quantitative imaging of intracellular ROS levels and redox status in rat hippocampal neurons. *NeuroImage* **54**:4, 2590-2602. [CrossRef]
2. Sanae Haga, Naoki Morita, Kaikobad Irani, Masato Fujiyoshi, Tetsuya Ogino, Takeaki Ozawa, Michitaka Ozaki. 2010. p66Shc has a pivotal function in impaired liver regeneration in aged mice by a redox-dependent mechanism. *Laboratory Investigation* **90**:12, 1718-1726. [CrossRef]
3. Andreas J. Meyer , Tobias P. Dick . 2010. Fluorescent Protein-Based Redox Probes. *Antioxidants & Redox Signaling* **13**:5, 621-650. [Abstract] [Full Text] [PDF] [PDF Plus]